Mitigation of Inrush Currents in Network Transformers by Reducing the Residual Flux With an Ultra-Low-Frequency Power Source

Baris Kovan, Francisco de León, *Senior Member, IEEE*, Dariusz Czarkowski, *Member, IEEE*, Zivan Zabar, *Senior Member, IEEE*, and Leo Birenbaum, *Senior Member, IEEE*

Abstract—**A methodology for the reduction of the residual flux in network transformers is proposed in this paper. The purpose is the mitigation of large inrush currents taken by numerous transformers when a long feeder is energized. Time-domain simulations are used to prove that a small-power device can substantially reduce the residual flux of all transformers simultaneously. The device consists of a low-voltage dc source, a suitable power-electronic switching unit, and a simple controller. Before a feeder is re-energized, the residual flux is reduced to a minimum and, as a consequence, the large inrush currents are reduced to an acceptable level. This greatly enhances the probability for the feeder to be successfully energized when otherwise a false trip would have occurred. Inrush current reductions of more than 60% are obtained at the head of the feeder.**

Index Terms—**Inrush currents, mitigation of inrush currents, residual flux reduction, transformers.**

I. INTRODUCTION

TRANSFORMER energization at no load may result in a very high inrush current. The peak value of the inrush current is a function of the switching instant of the terminal voltage, the characteristics of the hysteresis curve (residual and saturation fluxes), the primary winding resistance, and the inherent primary winding air-core inductance. Inrush currents are originated by the high saturation of the iron core during switching in. Excellent physical explanations of the phenomenon can be found in [1] and [2]. The driving force of the inrush current is the voltage applied to the primary of the transformer. The voltage may drive the flux to build up to a maximum theoretical value of twice the steady-state flux plus any residual flux. This super-saturation of the core may lead to an inrush current hundreds of times larger than the normal excitation current and many times larger than the rated current.

There are three negative side effects of inrush currents: 1) the protective devices for overloads and internal faults may falsely operate and disconnect the transformer. References [3]–[11] are
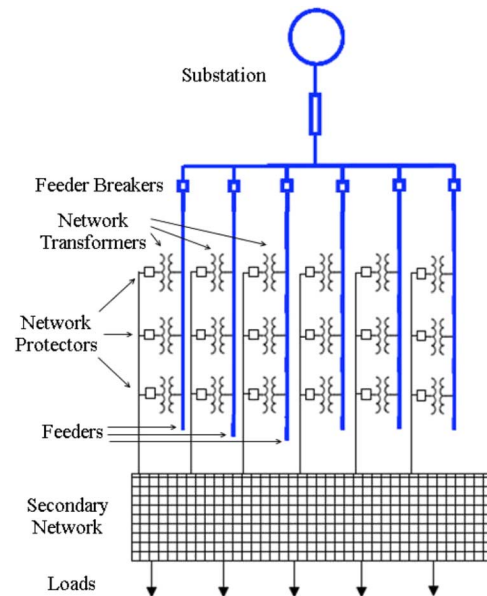
Fig. 1. Distribution network with substation and network transformers. The network transformers are 500-kVA three-phase Δ-Yg.

examples of the available techniques for relays to distinguish between faults and inrush currents used to reduce the number of undesirable trips; 2) the windings are exposed to mechanical stresses that can damage the transformer [12]–[14]; and 3) power-quality problems may arise: high resonant harmonic overvoltages [15] and voltage sags [16].

In an electric distribution network, when a feeder is energized following maintenance work, many parallel-connected network transformers draw inrush currents simultaneously. The purpose of this paper is to demagnetize "network transformers" [17], which are connected differently from (radial) "distribution transformers" [18]. The load of a radial distribution transformer remains connected when the transformer or feeder is offline. Therefore, the power to the loads (customers) is lost. In contrast, in networked systems, the secondaries of all network transformers, of different HV feeders are tied to each other through the low-voltage network. Therefore, when a feeder breaker is open, the associated network protectors to the transformers open (effectively isolating the feeder; that means, all network transformers are left open-circuited). As a result, in secondary networks, all loads are automatically re-routed and no disruption is felt by the customers. Take, for example, the circuit of Fig. 1; when one of the feeder breakers
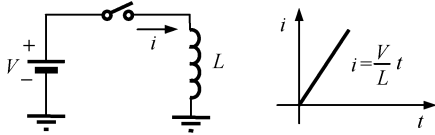
Fig. 2.   Current behavior in an inductive load fed by a dc source.
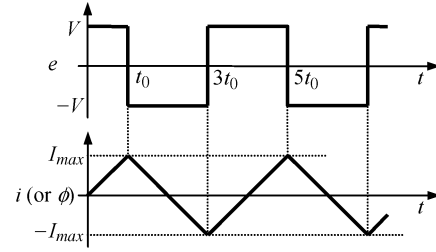

Fig. 3.   Current (flux) in the inductor fed by a square-wave voltage.
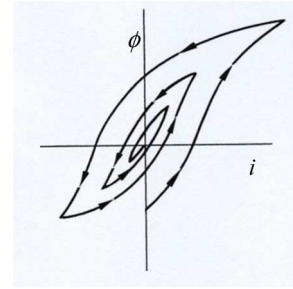

Fig. 4.   Hysteresis loops during demagnetization.
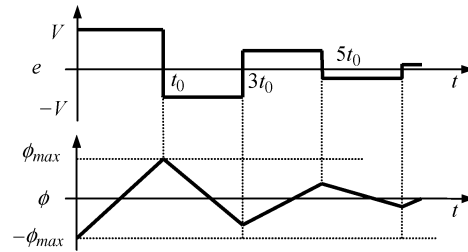

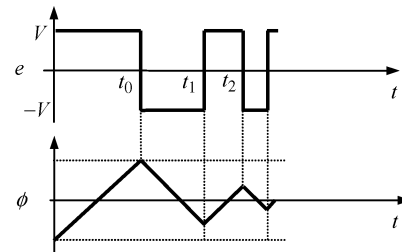Fig. 5.   Demagnetizing with variable voltage and constant frequency.

Fig. 6.   Demagnetizing with variable frequency and constant voltage.

closes, all transformers connected to that feeder are at no load and draw inrush currents. This is of great concern to power utilities because power restoration may fail. Not only can large inrush currents cause improper operation of protective relays, but they stress the transformer windings unduly or produce unacceptable voltage sags. As suggested in Fig. 1, our study is limited to the Δ-Yg transformer connection because it is the one most commonly used in networked systems.

A gamut of techniques aimed to reduce (or control) the magnitude of the inrush currents exists; see, for example, [19]–[25]. They can be divided into three groups: 1) methods that control the switching time (or angle) [19]–[21]; 2) methods that change the transformer design [22]–[24]; and 3) methods that reduce the residual flux [25], [26]. The latter, explored in this paper, can be a very effective way to reduce the inrush currents.

Dick and Watson [26] in 1981 used a low-power low-frequency power supply to characterize the core of power transformers, one at a time. The method was used to systematically demagnetize transformer cores with the aim of obtaining and modeling the behavior of the hysteresis loop (including minor loops). In this paper, we use the same technique to reduce the residual flux of many transformers connected to a medium-voltage feeder. Our demagnetizing device consists of a low-voltage dc source, a power-electronics switch, and a simple controller.

Simulations performed on a medium-voltage (MV) feeder (class 25 kV) having forty 500-kVA network transformers distributed evenly along its length are conducted to show the effectiveness of the method. We are able to simultaneously demagnetize all network transformers connected to the feeder and reduce the inrush currents by more than 60% with a 20-V, 2-kW ultra-low-frequency source.

II. DEMAGNETIZING TECHNIQUE

A. Response of an Inductor to DC Excitation

In agreement with Faraday's Law, when a dc voltage is applied to an inductor, a current $i(t)$ rises linearly with time at a rate given by the voltage applied to the inductance. The rise of current is illustrated in Fig. 2 and is expressed mathematically as

$$i(t) = \frac{1}{L} \int v(t) \cdot dt = \frac{V}{L} t. \qquad (1)$$

If, after a time $t = t_0$, when the current has reached a value of I_{max}, the voltage polarity is reversed, the current starts to decrease linearly at the same rate (see Fig. 3). If the voltage polarity is reversed again $2\,t_0$ later, at $t = 3\,t_0$, when the current has reached the value of $-I_{max}$, it will start increasing again. By iterating this voltage reversal process, the current will cycle as shown in Fig. 3. The flux in the linear inductor will have the same shape as the current in Fig. 3 because $\phi = L\,i$.

B. Variable Voltage — Constant Frequency (VVCF)

Consider that after disconnection, a transformer core has a residual flux as shown in Fig. 4. By gradually reducing successive dc voltage levels, each consecutive half-cycle would force a smaller voltage level onto the inductor. As a consequence, the flux ϕ in the inductor will be gradually reduced at each half-cycle; see Fig. 5.

Demagnetization is only achieved if, during the voltage reversal process, the path followed by the flux (ϕ) crosses the abscissa axis (i) each time by a smaller amount; see Fig. 4. To start the process, the core is taken into positive saturation by applying $+V$ for a time t_0. Then, the voltage is reversed and reduced successively.
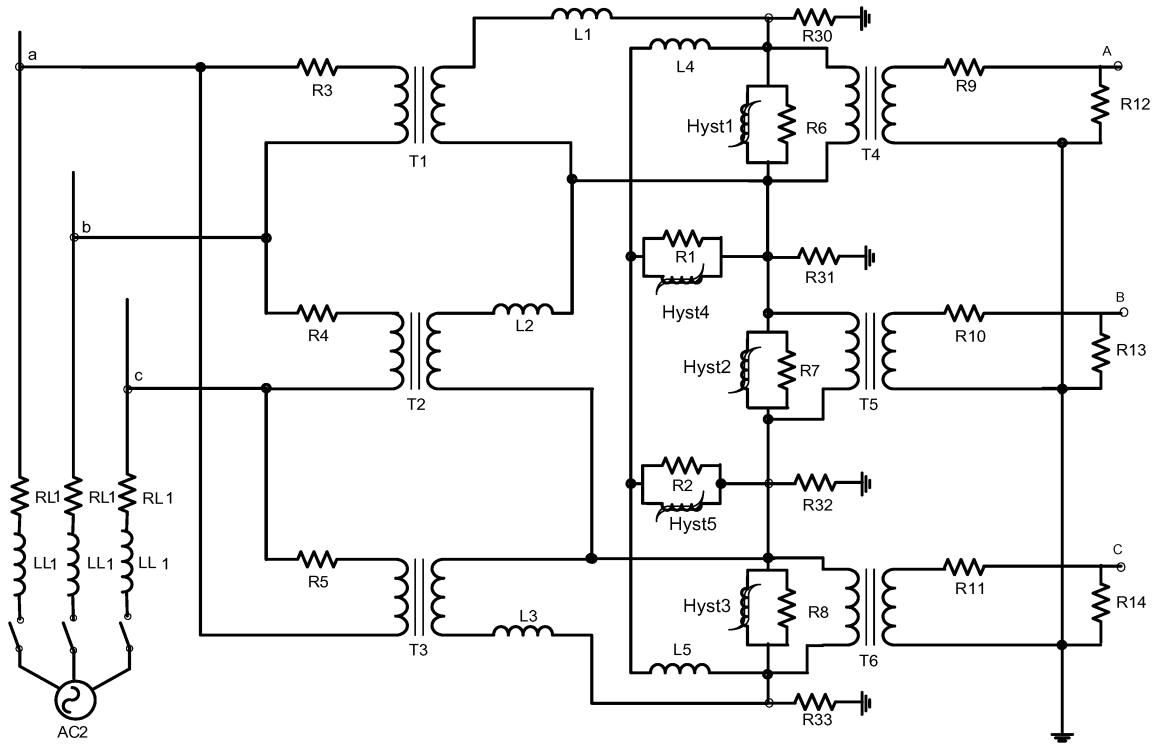
Fig. 7. Transformer model for time-domain simulations.

C. Variable Frequency — Constant Voltage (VFCV)

Demagnetization can also be achieved by keeping the voltage level constant, but gradually increasing the frequency of voltage reversal. That is, if the time interval between successive voltage reversals is gradually decreased, the amplitude of the flux ϕ in the inductor will also gradually decrease. See Fig. 6 for an illustration of the demagnetizing process of the VFCV technique. The key to the success of the VFCV approach is to deliver the same flux as the VVCF method. This is achieved by keeping the same area under the $V - t$ curve. To begin the process, the length of time (t_0) that the voltage is applied can be computed from the flux given by the area under the $V - t$ curve. See Section VI for the details of the switching strategy.

Both demagnetizing techniques (VVCF and VFCV) are equally effective in eliminating the residual flux of a hysteretic inductor. However, the VFCV has two advantages over the VVCF:

1) The physical realization with power-electronics converters and available voltage sources is substantially simpler.
2) The elimination of the residual flux is obtained in a shorter time.

III. COMPUTATION OF INRUSH CURRENTS

Inrush currents are computed in this paper with time-domain simulations using the EMTP-RV software. The simulations were performed so as to produce the worst possible inrush currents for the phase with highest residual flux. The switching angle was selected to be at $0°$ so that flux builds in the direction of the residual flux. Therefore, we always obtain twice the normal flux plus any residual flux on the leg. The transformer model, improved from [27], is derived from the principle of

TABLE I
PARAMETERS OF THE CIRCUIT OF FIG. 7

Circuit Elements	Value
L1, L2, L3	3.27 μH
L4, L5	10 μH
R1, R2	47 Ω
R3, R4, R5	5.75 Ω
R6, R7, R8	55.15 Ω
R9, R10, R11	0.37 mΩ
R12 to R14; R30 to R33	1 MΩ
T1, T2, T3	25:0.120
T4, T5, T6	1:1

duality to account for the core topology in a physical way. The model, illustrated in Fig. 7, includes the following items. The values are given in Table I.

1) Core topology represented by the hysteretic inductors Hyst1 through Hyst5. Their nonlinear behavior is described by the $\phi - i$ curve illustrated in Fig. 8.
2) Eddy current losses in the core are accounted for by resistors R1, R2, R6, R7, and R8 in parallel with the nonlinear hysteretic inductors.
3) Leakage and stray fluxes. Leakage flux is represented by inductors L1, L2, and L3. Inductors L4 and L5 represent the stray flux external to the windings.
4) Resistors R3, R4 and R5 represent the resistance of the high-voltage side windings, while R9, R10, and R11 represent the resistance of the low-voltage side windings.
5) Large resistors R12–R14 and R30–R33 are used to establish a ground reference and prevent numerical instabilities with the nonlinear inductors.
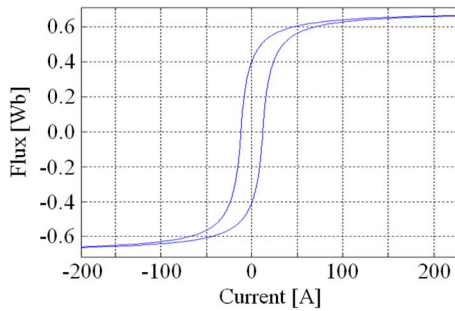
Fig. 8. Hysteresis curve for nonlinear inductors Hyst1 to Hyst5 in Fig. 7 (referred to one secondary).

Fig. 9. (a) Demagnetization circuit for a single-phase transformer. (b) Single-phase transformer model.

The differences between the model in [27] and the one shown in Fig. 7 are as follows.

1) The capacitors were omitted, since we are concerned with low-frequency phenomena. The results when including the capacitances between windings and to ground showed no detectable differences. This is in perfect agreement with the recommendations of [28].

2) Resistors R1–R14 and R3–R33 were introduced, as indicated in 5) above, to prevent numerical instabilities with the nonlinear inductors.

The model of the hysteresis characteristics of the core is very important to obtain the correct results. Fig. 8 shows the simulated hysteresis curve with a remanence of 0.4 Wb and a saturation level of about 0.65 Wb. Its coercive current is 12 A. To obtain a proper model, some of the fitting (default) parameters of the hysteretic reactor in the EMTP-RV had to be changed. It has been reported that the model of hysteretic reactors in EMTP-RV, when applied to the study of ferroresonance in voltage transformers, does not accurately represent the minor loops [29]. In [29], the more precise and physically sound model, based in the Preisach theory, is favored. However, in practice, the parameters of this model are very difficult to obtain for transformers installed and in operation perhaps for longer than 50 years.

IV. DEMAGNETIZING ONE TRANSFORMER

A. Single-Phase Transformer

In this section, we show with time-domain simulations using the EMTP that the residual flux of a transformer core can be eliminated with the technique (VFCV) described before. Fig. 9(a) shows the connection arrangement for a 167-kVA single-phase transformer. The transformer is represented by: 1) the winding resistance and half the leakage inductance in series and 2) the shunt magnetizing elements: a hysteretic inductor connected in parallel with a resistor representing the eddy current losses. The model, shown in Fig. 9(b), can be visualized as one of the three phases of the three-phase transformer shown in Fig. 7. The values of the parameters are also those of Table I.

In Fig. 10, we show the applied voltage together with the current and flux during the demagnetization process. One can see how the flux starts from the residual flux at −0.38 Wb. Regardless of what the residual flux is, the objective of the first voltage step is to drive the transformer into positive saturation. This is to
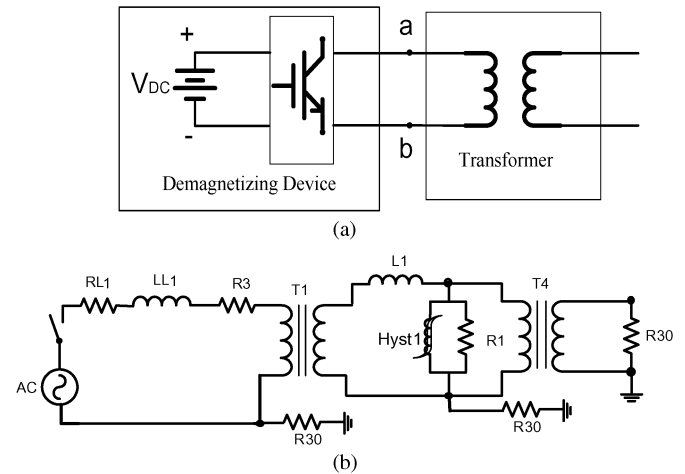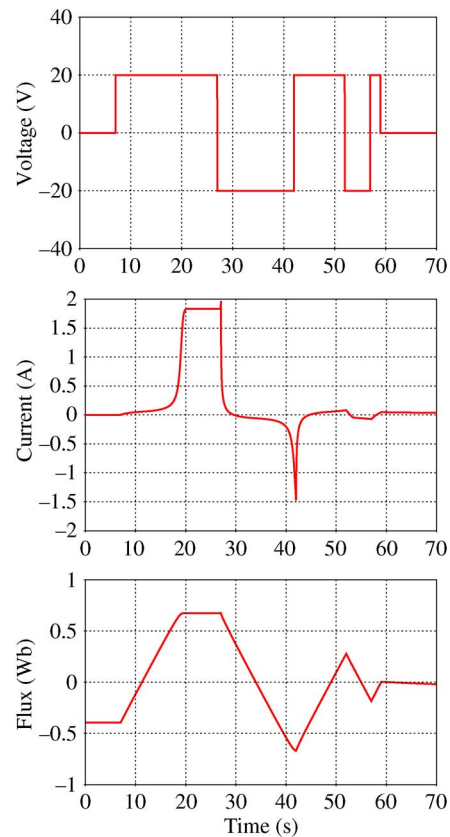

Fig. 10. Voltage, current, and flux during the demagnetization process of a single-phase transformer.

establish a reference point from where the demagnetizing technique can start. Subsequent voltage steps reduce the flux slowly to virtually zero.

In Fig. 11, we compare the inrush currents for the worst case scenario, given when a single-phase transformer is energized at the voltage zero crossing and the residual flux is at the maximum, against the case of no residual flux when it is energized at the voltage zero crossing. The peak current when maximum residual flux is present is close to 550 A (58 p.u.) while the peak
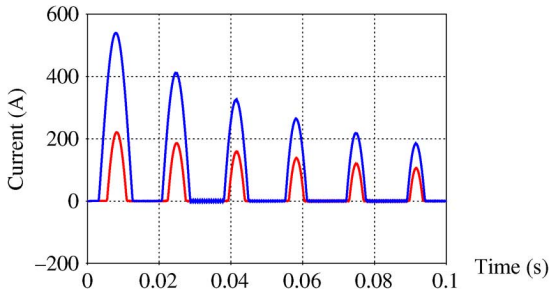
Fig. 11. Comparison of maximum inrush current with and without residual flux.
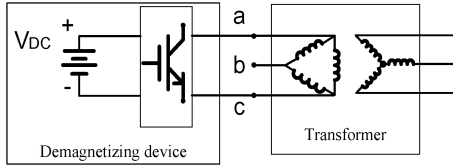

Fig. 12. Demagnetization circuit for a three-phase transformer.

current with zero residual flux is only 210 A (22 p.u.). Therefore, substantial improvement can be obtained when the residual flux is eliminated. Inrush currents have been reduced by 60% by eliminating the residual flux.
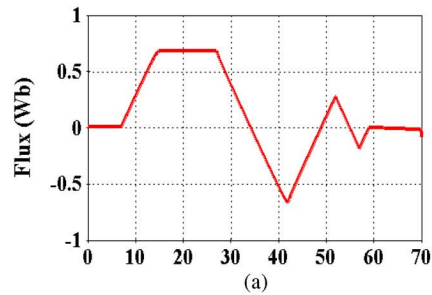
B. Three-Phase Transformer

Fig. 12 shows the circuit used to demagnetize a 500-kVA three-phase transformer. It can be seen that only one voltage source (20 V_{DC}) is needed. The source is connected between two phases with the other one left open. The waveforms for the voltage and current are similar to those shown in Fig. 10. The sole difference is that the first current peak becomes 2.6 A instead of 1.8 A, as in Fig. 10.

After applying the mitigation procedure, the residual flux was reduced in all five components. Compare the initial and final values of flux in Fig. 13. Before the application of the demagnetizing technique, the maximum residual flux [Fig. 13(a)] was -0.409 Wb in branch Hyst4. After demagnetizing the core, the maximum absolute residual flux is 0.095 Wb [Fig. 13(c) and (e)] in branches Hyst3 and Hyst5.

Table II shows the effect of the dc mitigation technique on the inrush currents. The inrush currents values correspond to the first peak of the simulations. It is seen that the inrush currents in the three phases were reduced by 76%, 98%, and 76% when compared to those without prior demagnetization.

As stated in the Introduction, the method presented here is based on the known principle that demagnetization of an iron core can be achieved by repeatedly reversing the voltage at the terminals of the device, while, at the same time, steadily decreasing its magnitude. At utility frequencies, 50 or 60 Hz, the power supply to perform the demagnetizing task is relatively large. The novel idea of this paper is the use of an ultra-low-frequency power supply, which leads to a much smaller power requirement.
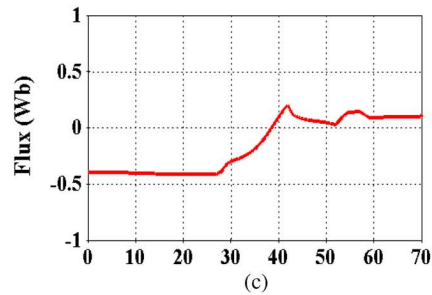
The rating of the new demagnetizing source may be estimated, conservatively, by assuming constant dc voltage and current; thus, 20 V × 2.6 A gives 52-W power. To put it in perspective, for a 500-kVA transformer, at 0.3% no-load current,
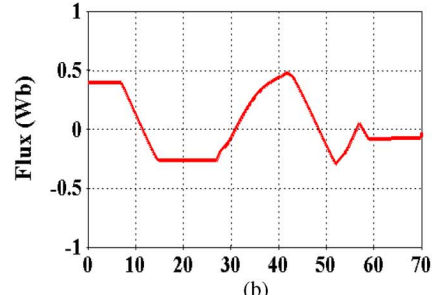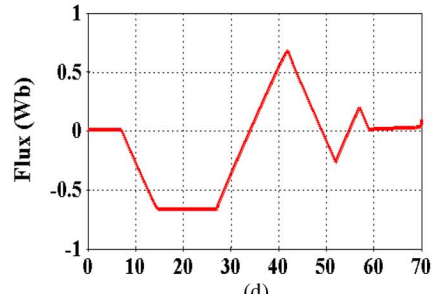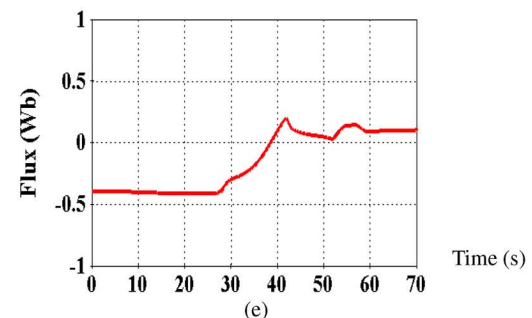
Fig. 13. Flux variation as the demagnetizing technique is applied to a three-phase transformer. (a) Hyst1, (b) Hyst2, (c) Hyst3, (d) Hyst4, (e) Hyst5.

operating at 60 Hz, a classical variac solution would require 1500 VA to achieve the same mitigation effect (i.e., the power requirement for the new technique is 3.5% of that for a 60-Hz unit). In the extreme case, when the transformer is fully saturated, the current will be limited only by the winding's resistance. For the delta connection, we see that the resistance seen

TABLE II
COMPARISON OF INRUSH CURRENTS FOR A
THREE-PHASE TRANSFORMER

Phase	Max Inrush Current before DC Mitigation [A]	Max. Inrush Current after DC Mitigation [A]
A	767	184
B	251	− 3.2
C	− 767	− 184

TABLE III
COMPARISON OF INRUSH CURRENTS TAKEN BY THE CONNECTION
OF 40 NETWORK TRANSFORMERS

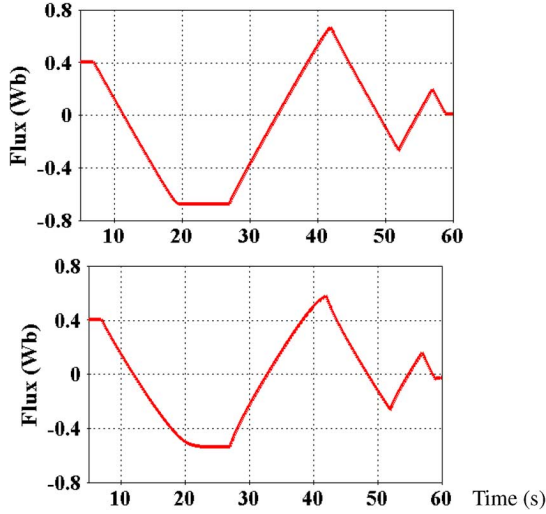| Phase	Before Mitigation [kA]	After Mitigation [kA]
A	− 3.48	− 1.42
B	− 0.68	1.10
C	− 3.49	1.43

Fig. 14. Variation of the flux in the leg Hyst1 of transformers 1 (top) and 38 (bottom) of the feeder during the demagnetizing process.

Fig. 15. Functional diagram of the demagnetizing device.

by the demagnetizing device is $(2/3)(5.75\Omega) = 3.83\Omega$; thus, for a 20-V source, the current drawn will be 5.2 A. Hence, for the worst possible case, the required power for demagnetizing will be 104 W or 7% of the variac alternative.

V. DEMAGNETIZING ALL TRANSFORMERS IN A FEEDER

In principle, it may be possible to demagnetize the entire set of open-circuited network transformers connected to the feeder, provided that the dc voltage magnitude, the initial reversal period, and the rate at which the period decreases are properly chosen. The case under study is illustrated in Fig. 1.

A constant amplitude (20 V), ultra-low-frequency (duration of the first half cycle is about 28 s, corresponding to 0.018-Hz frequency), rectangular dc voltage, of gradually increasing frequency, was applied to a feeder connected to 40 identical 500-kVA network transformers. We found that it is possible to demagnetize all of the transformers of a feeder with a single device connected, as shown in Fig. 12 at the head of the feeder. The plots in Fig. 14 illustrate the flux in one of the legs of the 1st and 38th transformers. The plots show that after about 60 s, the flux is 0.05 Wb or less. Note that the flux in transformer 38 is slightly smoother. This is because the impedance between the source and the transformer increases. The flux in all other transformers has very similar demagnetizing shapes.

We have noted that not all of the core fluxes reduce to zero (final points in Fig. 13). However, the inrush currents are still reduced substantially. Table III compares the results of the simulation of the inrush currents with and without the demagnetizing technique. After mitigation was applied to the feeder, the peak

values of the inrush currents in phases A and C were reduced by about 60% when compared with the values without mitigation. Note, however, that the inrush current in phase B has increased. This creates no problem because the inrush current of phase B is still smaller than that of the other two phases even after mitigation.

The power necessary to demagnetize the feeder would be 40 times the power for a single three-phase transformer, yielding approximately 2 kW (4 kW for the extreme fully saturated case). It is noted that in a real situation, all of the transformers connected to a feeder would not be identical, nor would the initial residual fluxes be identical, nor would they be equally spaced along the feeder. We intend to report in a sequel to this paper experimental results including a more accurate rating of the ultra-low-frequency power source.

VI. DEMAGNETIZING DEVICE AND STRATEGY

Demagnetization is achieved if during the voltage reversal process the path followed by the flux density (B) curve crosses the abscissa (H) axis. The measure as to how long the voltage in a given direction needs to be applied is the area under the $V - t$ curve, which is equal to the flux. One possible strategy will be presented.

The demagnetizing device consists of a low power, low-voltage dc source controlled by a power-electronics switch. Fig. 15 shows the functional electrical diagram. A double-pole double-throw switch is used to change the direction of the dc voltage to generate the required applied voltage to the transformer. The steps to demagnetize a core are as follows.

1) Bring the core to saturation by applying a positive V_{DC} voltage. This step is needed because the initial residual flux (ϕ_{res}) is not known. The indication that the core has reached (positive) saturation (ϕ_{sat}) is when the current stops increasing (point a in Fig. 16). However, this is detected some time later at point b.

2) Reverse the applied voltage (to negative V_{DC}) and measure the time that it takes for the core to be fully saturated in the reverse direction (point c in Fig. 16) detected a little later in point d. The time to bring the core from positive saturation to negative saturation is $t_c - t_b = \Delta t$. According
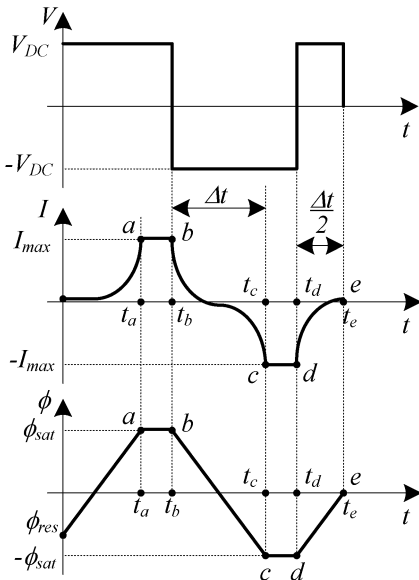
Fig. 16.   Demagnetizing strategy.

to Faraday's Law, the integral of the voltage from t_b to t_c gives a flux equal to twice the saturation flux

$$\int_{t_b}^{t_c} v(t)dt = V_{\mathrm{DC}}(t_c - t_b) = V_{\mathrm{DC}}\Delta t = 2\phi_{\mathrm{sat}}. \tag{2}$$

3) Reverse the voltage once again to apply positive V_{DC}. Theoretically, if we apply the voltage for a time equal to $\Delta t/2$ starting from negative saturation $(-\phi_{\mathrm{sat}})$, the core would be completely demagnetized (point e in Fig. 16).

The demagnetizing circuit realization cannot be based on mechanical switches (as shown in Fig. 15) because severe transient voltage stresses would occur by abruptly interrupting inductive currents. The actual circuit is based on power-electronic switches, including freewheeling diodes that prevent magnetic currents from being chopped abruptly; see [30].

VII. CONCLUSION

This paper has presented a technique to mitigate large inrush currents via the reduction of the residual flux in the core of transformers. The reduction in residual flux is achieved with a low-power ultra-low-frequency voltage source. The special power source produces a single-phase rectangular voltage waveform. This source is connected between two of the three-phase terminals at the head of the feeder. Rather than reducing the voltage as in the traditional demagnetizing technique, we have increased the frequency of voltage reversing. Therefore, the demagnetizing device consists of a low-voltage constant dc source, a power-electronics switch, and a simple controller.

With time-domain simulations on a single-phase transformer, we have illustrated the principle of operation. Simulations on a 25-kV feeder having 40 network transformers distributed along its length were conducted to show the benefits of the method. When the mitigation technique was used, the inrush currents calculated at the head of the feeder were reduced by about 60%. The power requirement of this new mitigation technique was shown to be about 2 kW (4 kW in extreme circumstances).

REFERENCES

[1] A. Greenwood, "Abnormal switching transients," in *Electrical Transients in Power Systems*, 2nd ed.   New York: Wiley, 1991, ch. 5, sec. 5.5, pp. 113–116.

[2] P. C. Y. Ling and A. Basak, "Investigation of magnetizing inrush current in a single-phase transformer," *IEEE Trans. Magn.*, vol. 24, no. 6, pp. 3217–3222, Nov. 1988.

[3] D. Q. Bi, X. A. Zhang, H. H. Yang, G. W. Yu, X. H. Wang, and W. J. Wang, "Correlation analysis of waveforms in nonsaturation zone-based method to identify the magnetizing inrush in transformer," *IEEE Trans. Power Del.*, vol. 22, no. 3, pp. 1380–1385, Jul. 2007.

[4] J. Faiz and S. Lotfi-Fard, "A novel wavelet-based algorithm for discrimination of internal faults from magnetizing inrush currents in power transformers," *IEEE Trans. Power Del.*, vol. 21, no. 4, pp. 1989–1996, Oct. 2006.

[5] P. L. Mao and R. K. Aggarwal, "A wavelet transform based decision making logic method for discrimination between internal faults and inrush currents in power transformers," *Elect. Power Energy Syst.*, vol. 22, no. 6, pp. 389–395, Aug. 2000.

[6] M. A. Rahman and B. Jeyasurya, "A state-of-the-art review of transformer protection algorithms," *IEEE Trans. Power Del.*, vol. 3, no. 2, pp. 534–544, Apr. 1988.

[7] P. Liu, O. P. Malik, C. Chen, G. S. Hope, and Y. Guo, "Improved operation of differential protection of power transformers for internal faults," *IEEE Trans. Power Del.*, vol. 7, no. 4, pp. 1912–1919, Oct. 1992.

[8] T. S. Sidhu, M. S. Sachdev, H. C. Wood, and M. Nagpal, "Design, implementation and testing of a microprocessor-based high-speed relay for detecting transformer winding faults," *IEEE Trans. Power Del.*, vol. 7, no. 1, pp. 108–117, Jan. 1992.

[9] K. Inagaki and M. Higaki, "Digital protection method for power transformers based on an equivalent circuit composed of inverse inductance," *IEEE Trans. Power Del.*, vol. 4, no. 4, pp. 1501–1510, Oct. 1998.

[10] K. Yabe, "Power differential method for discrimination between fault and magnetizing inrush current in transformers," *IEEE Trans. Power Del.*, vol. 3, no. 3, pp. 1109–1117, Jul. 1997.

[11] T. S. Sidhu and M. S. Sachdev, "Online identification of magnetizing inrush and internal faults in three-phase transformers," *IEEE Trans. Power Del.*, vol. 7, no. 4, pp. 1885–1891, Oct. 1992.

[12] M. Steurer and K. Fröhlich, "The impact of inrush currents on the mechanical stress of high voltage power transformer coils," *IEEE Trans. Power Del.*, vol. 17, no. 1, pp. 155–160, Jan. 2002.

[13] J. Faiz, B. M. Ebrahimi, and T. Noori, "Three- and two-dimensional finite-element computation of inrush current and short-circuit electromagnetic forces on windings of a three-phase core-type power transformer," *IEEE Trans. Magn.*, vol. 44, no. 5, pp. 590–597, May 2008.

[14] A. A. Adly, "Computation of inrush current forces on transformer windings," *IEEE Trans. Magn.*, vol. 37, no. 4, pp. 2855–2857, Nov. 2001.

[15] D. Povh and W. Schultz, "Analysis of overvoltages caused by transformer magnetizing inrush current," *IEEE Trans. Power App. Syst.*, vol. PAS-97, no. 4, pp. 1355–1365, Jul. 1978.

[16] M. Nagpal, T. Martinich, A. Moshref, K. Morison, and P. Kundur, "Assessing and limiting impact of transformer inrush current on power quality," *IEEE Trans. Power Del.*, vol. 21, no. 2, pp. 890–896, Apr. 2006.

[17] *IEEE Stand. Terminology For Power and Distribution Transformers*, IEEE Std. C57.12.80-2002, 2002, p.22, 3.269.

[18] *IEEE Stand. Terminology For Power and Distribution Transformers*, IEEE Std. C57.12.80-2002, 2002, p.9, 3.105.

[19] O. A. Mahgoub, "Microcontroller-based switch for three-phase inrush current minimization," in *Proc. IEEE Int. Power Electron. Congr.*, Cuernavaca, Mexico, 1996, pp. 107–112.

[20] J. H. Brunke and K. J. Frohlich, "Elimination of transformer inrush currents by controlled switching, part I: Theoretical considerations," *IEEE Trans. Power Del.*, vol. 16, no. 2, pp. 276–280, Apr. 2001.

[21] J. H. Brunke and K. J. Frohlich, "Elimination of transformer inrush currents by controlled switching, part II: Application and performance considerations," *IEEE Trans. Power Del.*, vol. 16, no. 2, pp. 281–285, Apr. 2001.

[22] J. F. Chen, T. J. Liang, C. K. Cheng, S. D. Chen, R. L. Lin, and W. H. Yang, "Asymmetrical winding configuration to reduce inrush current with appropriate short-circuit current in transformer," *Proc. Inst.Elect., Eng., Elect. Power Appl.*, vol. 152, no. 3, May 2005.

[23] V. Molcrette, J. Kotny, J. Swan, and J. Brudny, "Reduction of inrush current in single-phase transformer using virtual air gap technique," *IEEE Trans. Magn.*, vol. 34, no. 4, pp. 1192–1194, Jul. 1998.

[24] C. K. Cheng, T. J. Liang, J. F. Chen, S. D. Chen, and W. H. Yang, "Novel approach to reducing the inrush current of a power transformer," *Proc. Inst. Elect. Eng., Elect. Power Appl.*, vol. 151, no. 3, pp. 289–295, May 2004.

[25] F. W. Sears, "Ferromagnetism," in *Electricity and Magnetism*. Reading, MA: Addison-Wesley, 1951, ch. 15, sec. 15-3, pp. 335–339.

[26] E. P. Dick and W. Watson, "Transformer models for transient studies based on field measurements," *IEEE Trans. Power App. Syst.*, vol. PAS-100, no. 1, pp. 409–419, Jan. 1981.

[27] B. A. Mork, F. Gonzales, D. Ishchenko, D. L. Stuehm, and J. Mitra, "Hybrid transformer model for transient simulation-part I: Development and parameters," *IEEE Trans. Power Del.*, vol. 22, no. 1, pp. 248–255, Jan. 2007.

[28] CIGRE Working Group 02 (SC 33), Guidelines for representation of network elements when calculating transients, CIGRE Tech. Brochure 39, 1990.

[29] A. Rezaei-Zare, R. Iravani, M. Sanaye-Pasand, H. Mohseni, and S. Farhangi, "An accurate hysteresis model for ferroresonance analysis of a transformer," *IEEE Trans. Power Del.*, vol. 23, no. 3, pp. 1448–1456, Jul. 2008.

[30] M. H. Rashid, *Power Electronics — Circuits, Devices, and Applications*, 3rd ed. Upper Saddle River, NJ: Prentice-Hall, 2004, ch. 6, p. 232, Fig. 6.2.

Baris Kovan was born in Ankara, Turkey, in December 1980. He received the B.Sc. and the M.Sc. (Hons.) degrees in electrical engineering from Polytechnic Institute, New York University Honors College, Brooklyn, NY, in 2008.

He was an Intern in the utility and construction fields. Currently, he is with Altran Solutions. His career and research interests are renewable energy and distributed generation.

Francisco de León (S'86-M'92-SM'02) received the B.Sc. and M.Sc. degrees in electrical engineering from the National Polytechnic Institute, Mexico, in 1983 and 1986, respectively, and the Ph.D. degree from the University of Toronto, Toronto, ON, Canada, in 1992.

He has held several academic positions in Mexico and has worked for the Canadian electric industry. Currently, he is an Associate Professor at the Polytechnic Institute of New York University, Brooklyn, NY. His research interests include the analysis of power phenomena under nonsinusoidal conditions, the transient and steady-state analyses of power systems, the thermal rating of cables, and the calculation of electromagnetic fields applied to machine design and modeling.

Dariusz Czarkowski (M'97) received the M.S. degree in electronics from the University of Mining and Metallurgy, Cracow, Poland, in 1989, the M.S. degree in electrical engineering from Wright State University, Dayton, OH, in 1993, and the Ph.D. degree in electrical engineering from the University of Florida, Gainesville, in 1996.

In 1996, he joined the Polytechnic University, Brooklyn, NY (now Polytechnic Institute, New York University), where he is currently an Associate Professor of Electrical and Computer Engineering. He is a coauthor of *Resonant Power Converters* (Wiley, 1995). His research interests are in power electronics, electric drives, and power quality.

Zivan Zabar (M'76–SM'81) was born in Hadera, Israel, in 1939. He received the B.Sc., M.Sc., and D.Sc. degrees from the Technion-Israel Institute of Technology in 1965, 1968, and 1972, respectively.

Currently, he is a Professor of Electrical Engineering at the Polytechnic Institute, New York University, Brooklyn, NY. His areas of interest are linear propulsion, electrical power conversion systems, and power electronics. He has six patents and has had many papers published in technical journals. He is a member of Sigma Xi.
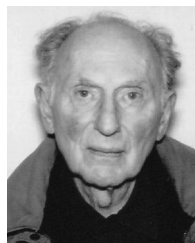
Leo Birenbaum (S'45–A'48–M'55–SM'70) was born in New York City in 1927. He received the B.E.E. degree from the Cooper Union in 1946, and the M.E.E. and M.S. (Phys) degrees from Polytechnic Institute, Brooklyn, NY, in 1958 and 1974, respectively.

Currently, he is Professor Emeritus at the Polytechnic Institute, where, for many years, he taught courses in electric circuits, electromechanical power conversion, electromagnetic fields, and rotating machinery. He has conducted research in a number of areas: microwave components and transmission, biological effects of microwave and low-frequency electromagnetic fields, electromagnetic launchers, and electric power distribution. He is a coauthor of approximately 40 peer-reviewed papers, and he holds 3 patents on microwave devices.

Prof. Birenbaum is a member of Sigma Xi, Tau Beta Pi, the BioElectroMagnetics Society, and the New York Academy of Sciences.